1992AJ....104.1000Z

THE ASTRONOMICAL JOURNAL VOLUME 104, NUMBER 3 SEPTEMBER 1992

UCM 2257+2438, A NEW NARROW-LINE SEYFERT 1 GALAXY[1]

J. ZAMORANO, J. GALLEGO, AND M. REGO

Departamento de Astrofísica, Universidad Complutense, 28040 Madrid, Spain

A. G. VITORES

Departmento de Astrofísica, Universidad Complutense, 28040 Madrid, Spain, and EUIT Industrial Universidad Politécnica, 28012 Madrid, Spain

R. GONZALEZ-RIESTRA

ESA-IUE Observatory, Villafranca Satellite Tracking Station, Spain

Received 31 January 1992; revised 21 April 1992

ABSTRACT

Multiwavelength observations of the galaxy UCM 2257+2438 found in the Universidad Complutense of Madrid (UCM) objective-prism survey are reported. The optic spectroscopy, CCD imaging, near-infrared and *IRAS* photometric data suggest that this object is a narrow-line Seyfert 1 placed in the nucleus of a Sa nearly face-on galaxy with a significant contribution from starlight.

1. INTRODUCTION

For the past four years we have been conducting an objective-prism survey of Hα emission-line galaxies in selected fields of the Northern Hemisphere, with the aim of finding low-metallicity galaxies. Details of the instrumentation, search techniques, and first results are given in Rego *et al.* (1989) and Zamorano *et al.* (1990). Although a large proportion of the extragalactic objects found are star-forming galaxies, there are some of them that, when analyzed from near-infrared or *IRAS* data, show evidence of activity. This is the case of UCM 2257+2438, which was found in the course of our survey. This galaxy was independently discovered by the survey of Kazarian & Kazarian (1980), who named it KAZ 320. The spectrum of KAZ 320 is described as sharp, stellarlike in appearance, and with moderate intensity in the continuum. Due to the nature of the survey for UV excess galaxies, they did not give any information about the presence of emission lines in the spectra of their objects. UCM 2257+2438, which is located 4 arcmin north of UGC 12290, also known as CGCG 457.015 and IRAS 22571+2434, does not appear either in the Dixon & Sonneborn (1980) compilation or in the *Catalogue of Principal Galaxies* (Paturel *et al.* 1989).

The low-resolution objective-prism spectrum (6400–6850 Å) of UCM 2257+2438 displays a weak continuum with a very strong emission-line feature. The contrast between line and continuum is an indicator of the equivalent width of the Hα+[N II] blend. This spectral feature was so conspicuous, that this object was classified among the strongest ones of the sample, a category which includes only 8% of all candidates selected. A measure of the equivalent width in the spectra taken with higher resolution yields EW (Hα+[N II])=315 Å and EW(Hα)=255 Å. Near-infrared and *IRAS* photometry provide evidence of the prevailing nonthermal nature of UCM 2257+2438. The spectrum taken at moderate resolution confirms this prediction and also reveals unusual features: forbidden emission lines from ions spanning a wide range of ionization and permitted lines slightly broader, superimposed on a featureless continuum. These are properties which lead to the classification of UCM 2257+2438 as a narrow-line Seyfert 1 galaxy according to Osterbrock & Pogge (1985).

In this paper we present optical spectrophotometry, CCD imaging, and near-infrared photometry of UCM 2257+2438 and then we use these data to address questions concerning the morphology, nature of the observed emission, and physical properties of the emission-line region. In addition, *IRAS* fluxes have been extracted in order to contrast previous results and to estimate the 60 μm luminosity of the *IRAS* counterpart.

2. OBSERVATIONS AND REDUCTIONS

2.1 Imaging

CCD images of UCM 2257+2438 were acquired with the 2.2 m telescope at the Calar Alto German–Spanish Observatory (Almería, in Spain) in 1989 June and 1990 December (see Table 1). In both runs the exposure time was 1800 s. The CCD chip used was a RCA of 640×1024 pixel, binned in both axis to a final pixel size of 30 μm, which is equivalent to 0.35 arcsec on the sky. Field coverage of the images is 2×3 arcmin. Both images were taken through a Gunn–Thuan *r* filter. Atmospheric conditions were photometric during both observing runs, but seeing was better in the 1990 observation (1.5 arcsec). Absolute calibration was obtained by observing, repeatedly during the night, a set of standard stars, taken from the list given by Kent (1985). High S/N ratio dome flats and exposures of the sky taken in twilight were also obtained. The standard procedure of bias removal, dark-current subtraction, and flat fielding using dome and sky flatfields was performed with the ESO image processing system (MIDAS).

[1]Based on observations taken at Calar Alto German–Spanish Observatory (Almería, Spain) and Izaña Observatory, Tenerife, Spain.

 0004-6256/92/091000-09$00.90 © 1992 Am. Astron. Soc. 1000

© American Astronomical Society • Provided by the NASA Astrophysics Data System

1992AJ....104.1000Z

TABLE 1. Journal of observations.

Photometry		
Telescope	Calar Alto 2.2 m	
Filter	Gunn–Thuan *r*	
Exposure time	1800 s	
Dates	1989 June	1990 December
Seeing	2.5 arcsec	1.5 arcsec
Total field	2×3 arcmin	
Pixel size	30 μm=0.35 arcsec	
Spectroscopy		
Telescope	Calar Alto 3.5 m	
Instrument	Twin Spectrograph	
Date	1989 November	
Exposure time	2700 s	
Slit width	2.35 arcsec	
Position angle	90° (E–W)	
Channel	Blue	Red
Chip	RCA 30 μm	GEC 22 μm
Grating	300 l/mm	400 l/mm
Dispersion	144 Å/mm	108 Å/mm
Scale	0.8 arcsec/pixel	1 arsec/pixel
Spectral coverage	4000–5000 Å	6000–7000 Å
Near-infrared data		
Telescope	Izaña IR 1.5 m	
Instrument	Oxford Photometer	
Date	1991 October	
Integration aperture	15 arcsec	
Position angle	90° (E–W)	

The image of the galaxy fills only a small portion of the frames and the sky background was flat to a level of 1–2%. Sky level is 21.0 mag/arcsec^2.

The contour isophotal map of the Gunn–Thuan *r* image of UCM 2257+2438 is presented in Fig. 1 in steps of 1 mag/arcsec.^{2} The lowest isophote represents 25 mag/arcsec^2. With the help of the program GASP (Davis *et al.* 1985) isophotes were fitted to ellipses. The brightness profile is plotted in Figs. 2(a) and 2(b). It is evident from Fig. 2(b) that the profile follows an $r^{1/4}$ law (de Vaucouleurs 1948), except near the center where seeing effects dominate. In Fig. 2(a), the solid line represents the best fit obtained by the summation of a bulge $r^{1/4}$ law (de Vacoucouleurs 1948) and an exponential disk law (Freeman 1970), using the procedure outlined in Schombert & Bothun (1987) and the Downhill Simplex Method (Neltzer & Mead 1965) to perform the minimization. No attempt has been made to fit the nuclear part of the galaxy where seeing smears the intrinsic light distribution. This simple bulge-disk decomposition produces the following set of parameters: central surface brightness $\mu_0=17.6$ mag/arcsec^2 and disk length $D_1=0.7$ arcsec for the disk, and effective surface brightness $\mu_e=20.5$ mag/arcsec^2, and effective radius $r_e=2.3$ arcsec for the bulge component.

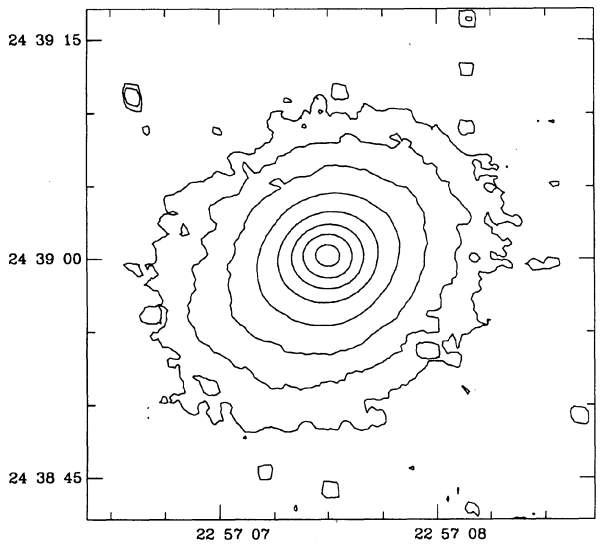

FIG. 1. Contour map of isophotes of UCM 2257+2438 in the Gunn–Thuan *r* band. Magnitude interval in steps of 1 mag/arcsec^2. The faintest isophote represents 25 mag/arcsec^2. The isophotes twisting is clearly apparent.

2.2 Spectrophotometry

Spectra at moderate resolution of UCM 2257+2438 were obtained in 1989 November at Calar Alto German–Spanish Observatory, with the twin spectrograph attached to the Cassegrain focus of the 3.5 m telescope (see Table 1). A slit of width 2.35 arcsec was placed centered on the nucleus and in the E–W direction, i.e., the position angle was P.A.=90°. During exposure the seeing fluctuated between 2 and 6 arcsec. The spectrograph has two channels which allow simultaneous observations of the blue and red spectra. In the blue, we used an RCA CCD detector with equivalent pixel size of 30 μm, together with a 300 g/mm grating, which provided a dispersion of 144 Å/mm (4.3 Å/pixel). The full width at half-maximum (FWHM) of the instrumental profile, as measured in the comparison arc spectra and in the night sky lines is 8.1 Å, i.e., 480 km s^{-1}. Although the wavelength coverage is larger, we could use only the range $\lambda\lambda$ 4000–5000 Å, due to the low efficiency of the RCA chip in the violet region. A GEC CCD detector with pixel size of 22 μm and a 400 g/mm grating was used for the red side, giving a linear dispersion of 108 Å/mm (1.84 Å/pixel) and a FWHM of the instrumental profile of 6.3 Å, i.e., 280 km s^{-1}. The available spectral range is from $\lambda\lambda$ 5950 to 7000 Å. The exposure time was 2700 s in both colors. The spatial scale was 0.8 and 1 arcsec/pixel in the blue and red channels, respectively.

Four standard stars, Hiltner 102, EG 247, BD +284211, and Hiltner 600, were observed at different airmasses in order to monitor the atmospheric extinction and ensure suitable flux calibration. The agreement between the response curves corresponding to the different standard stars is better than 10%. Reduction of the data were carried out using the MIDAS software package, and involves flatfielding, wavelength calibration, sky subtraction, extinction correction, and conversion to absolute fluxes.

2.3 Near-Infrared Data

The observations were made in 1991 October with the Oxford IR photometer coupled with the CSM 1.5 m telescope at Izaña Observatory (Tenerife, Spain). The galaxy

© American Astronomical Society • Provided by the NASA Astrophysics Data System

1992AJ....104.1000Z

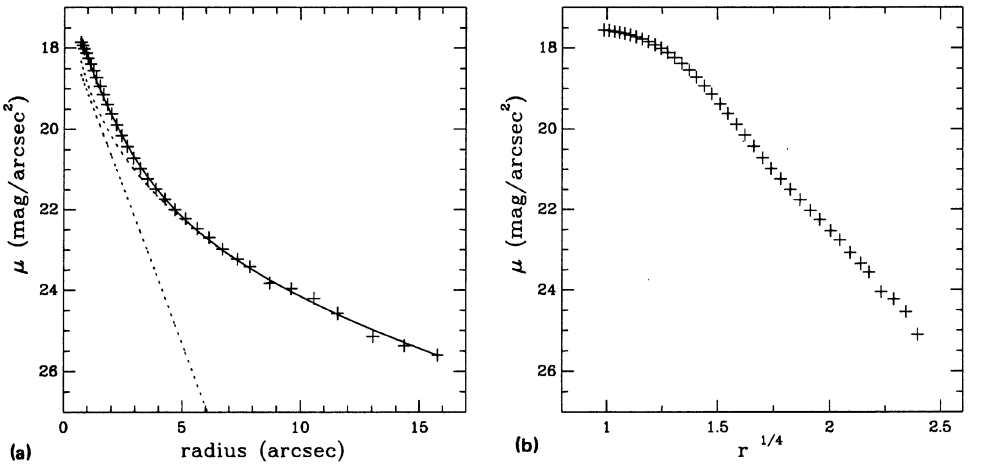

FIG. 2. (a) Brightness profile plotted against the mean radius. Solid line represents the best fit obtained as the summation of a $r^{1/4}$ law and an exponential disk law. (b) Brightness profile vs $r^{1/4}$. The bulge contribution is clearly prominent.

was observed through a single circular aperture of 15″ diam in the Johnson J (1.25 μm), H(1.65 μm), and K (2.2 μm) broadband filters. The chopping throw was 30 arcsec in the E–W direction. Reduction was performed by observing the stars HR 8905, HR 7244, and HR 1140 several times each night at comparable airmass to the object. The uncertainties resulting from repeated observations, each one consisting of consecutive integrations, represent the dominant source of error in the final magnitudes.

2.4 IRAS Data

As a first approach to study the far-infrared characteristics of our object, we searched the *IRAS* PSC catalog but no PSC counterpart was found at our optical position. The fact that nearly all UCM galaxies brighter than $m_B=15.0$ were found in the PSC suggested that coadding the original *IRAS* scans at the location of our galaxy would lead to the detection at least at the 60 μm band. The facilities of the Infrared Processing and Analysis Center (IPAC) at the Rutherford Appleton Laboratory (Oxford) were used to carry out the work. Because UCM 2257+2438 is a point source as seen by *IRAS* (diameter less than 2 arcmin), the data were coadded in a one-dimensional sense only. The output from the coadding routines was examined in detail in order to reject the too noisy scans. Possible contaminations from near sources were uncovered by examining plots of the accumulated data and by considering the values from each *IRAS* band. The resulting *IRAS* photometry is given in Table 2 and the contour plots of the region around the object at the four *IRAS* bands are shown in Fig. 6.

3. RESULTS

3.1 Emission Lines

The spectrum of UCM 2257+2438, as shown in Fig. 3, is the result of adding all the scans with significant signal in the emission lines along the slit, i.e., 14 arcsec. Due to the poor seeing during the spectroscopic observation, the light distribution is completely smeared and all attempts to obtain reliable spatial information have been fruitless. However, there is some evidence that the emission-line material is extended. Both starlight and emission gas are centered in the nucleus.

It exhibits strong Balmer, [O III] $\lambda\lambda$ 5007 and 4959 lines and some high ionized species like [Fe VII] λ6087 and [Fe X] λ6375 Å emission lines typical of a Seyfert 1 galaxy, on a featureless continuum. Permitted Fe II emission lines, if present, are too weak to be detected.

The redshift was computed as a weighted mean considering the redshifts of all measurable emission lines in the spectrum, using their equivalent widths as relative weight. The resulting value $z=0.0337\pm0.0001$, yields a distance of 200 Mpc, assuming $H_0=50$ km s^{-1} Mpc^{-1}.

Emission-line fluxes, given in Table 3, were measured using a 2° polynomial fit to the local continuum on either side of the line and integrating the continuum-subtracted flux over the line profile. The error in the line fluxes is always below 15%; the stronger lines have been measured with an accuracy better than 5%. In order to correct for

TABLE 2. General characteristics of UCM 2257+2438.

R.A. (1950.0)	22h 57m 07.5s
Dec(1950.0)	+24° 38′ 59″
Redshift	$z=0.0337\pm0.0001$
Distance	200 Mpc ($H_0=50$ km s^{-1} Mpc^{-1})
Gunn–Thuan r	15.88 ± 0.05
J	13.4 ± 0.2
H	12.6 ± 0.2
K	12.1 ± 0.1
IRAS flux 12 μm	$0.05L$
IRAS flux 25 μm	0.13 ± 0.07
IRAS flux 60 μm	0.45 ± 0.10
IRAS flux 100 μm	2.12 ± 0.74
Absolute Mag	$M_r=-20.9$
Type	Sa+Sy 1 nucleus
Diameter	14 arcsec↔14 kpc
E($B-V$)	0.54

© American Astronomical Society • Provided by the NASA Astrophysics Data System

1992AJ....104.1000Z

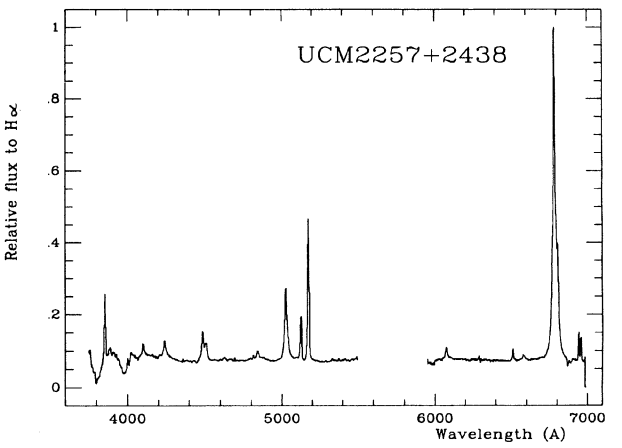

FIG. 3. The spectrum of UCM 2257+2438 is typical of Seyfert 1 galaxies with both broad and narrow Balmer H II emission lines and narrow forbidden lines. This galaxy exhibits a high degree of ionization as shown by the presence of [Fe X]λ6375.

reddening effects, values of the extinction coefficient $c(\mathrm{H}\beta)$ were computed for each couple of Balmer lines by assuming (Osterbrock 1989) typical values for Seyfert galaxies, $T_e = 10\,000$ K and $N_e = 10\,000$ cm^{-3}. The final value of $c = 0.77$ was attained weighting the different values, corresponding to a total reddening of $E(B-V) = 0.54$. The extinction due to our galaxy in the direction of UCM 2257 +2438 amounts to $E(B-V) = 0.15$ (Burstein & Heiles 1984). The reddening of the forbidden lines may be assumed to be the same, in spite of the difference in polarization properties (Koski 1978). The [O III] 5007/Hβ intensity ratio of 1.11 and the Balmer decrement Hα/Hβ of 5.3 are in the typical range observed in Seyfert 1 galaxies.

TABLE 3. UCM 2257+2438 emission-line fluxes relative to Hβ.

Ion	λ (Å)	F	F_c
[O II]	3727	406	668
[Ne III]	3869	96	147
[Fe V]	3893	282	429
[Ne III]	3967	63	93
[Fe V]*	4071	2	3
Hδ	4101	167	234
Hγ	4340	415	523
[O III]	4363	70	87
He I*	4471	4	5
[Fe III]	4658	189	208
He II	4686	55	60
Hβ	4861	1000	1000
[O III]	4959	369	350
[O III]	5007	1176	1092
[Fe VII]	5159	32	27
[Fe VI]	5176	22	18
[N I]*	5199	16	13
He I	5875	109	70
[Fe VII]	6087	24	15
[O I]	6300	74	42
[S III]*	6312	13	7
[O II]	6363	60	33
[Fe X]*	6375	4	2
[Fe X]*	6389	12	7
[N II]	6548	84	44
Hα broad	6563	4229	2194
Hα narrow	6563	1182	613
[N II]	6583	253	131
[S II]	6716	171	86
[S II]	6731	151	76

Notes to TABLE 3

$F(\mathrm{H}\beta) = 7.6\times10^{-15}$ erg cm^{-2} s^{-1}.
$F(\mathrm{H}\beta)_c = 5.5\times10^{-14}$ erg cm^{-2} s^{-1}.
*Dubious identification.

FWHMs were also measured. The observed Hβ and Hα FWHMs are 1100 and 690 km s^{-1}, respectively, and they are in all cases broader than the FWHM of the instrumental profile. The full widths at zero intensity (FWZI) measured are about 6000 km s^{-1} for both lines, although these values are difficult to measure with precision. These lines are not dramatically broader than the [O III] 5007 line, which has a FWHM of 590 km s^{-1}, leading to an average velocity dispersion of 250 km s^{-1} for the narrow region. These properties suggest that UCM 2257+2438 is more accurately classified as "narrow-line Seyfert 1" galaxy.

Note that the measured widths of Hβ and Hα are not the same. The difference, which is larger than the average errors of individual widths, occurs also in several Seyferts as Mk 79, Mk 141, Mk 142, Mk 236, and Mk 291, which belong to a sample of 35 Seyferts studied by Osterbrock (1977). Particularly, one of these objects, Mk 291, classified as a Seyfert 1, has Hβ and Hα FWHM values of 1100 and 500 km s^{-1}, respectively, near to that measured in UCM 2257+2438. This difference was interpreted by Osterbrock (1977) as being, at least in part, due to the relative proportions of the Hα and Hβ narrow and broad components or to real differences in the profiles, relating to different excitation rates in distinct regions of velocity space.

We have attempted to analyze the components of the Balmer lines using deblending routines available in the MIDAS package. As a first approach, broad and narrow components of each line were assumed to be Gaussians of different widths and no boundary conditions were settled. This procedure worked well for Hβ, yielding a narrow component of 600 km s^{-1} and a broad component of 1800 km s^{-1}. Both components are centered in 5027 $\pm$ 1 Å. For the Hα deblend, the [N II] lines possess an additional problem. Boundary conditions in this case were the relative positions of the lines and the intensity ratio of [N II] lines. The fit using Gaussians provided results as good as those obtained using scaled [S II] lines for the [N II] lines. Narrow and broad components for Hα are 360 and 1700 km s^{-1}, respectively. Figures 4(a) and 4(b) display the results of these fits. A cursory inspection shows the presence of relative strong wings in the Balmer lines.

We have constructed a mean profile for [O III] lines by adding observed profiles of [O III] 4959,5007 lines. The lines were normalized and shifted in the velocity field to the reference redshift of the galaxy. A blueward slanting asymmetry in this mean profile is clearly apparent [see Fig. 4(c)]. This asymmetry is not found in lines of low ionization species such as He I 5876 and [S II] 6716,6731 [Fig. 4(d)].

© American Astronomical Society • Provided by the NASA Astrophysics Data System

1992AJ....104.1000Z

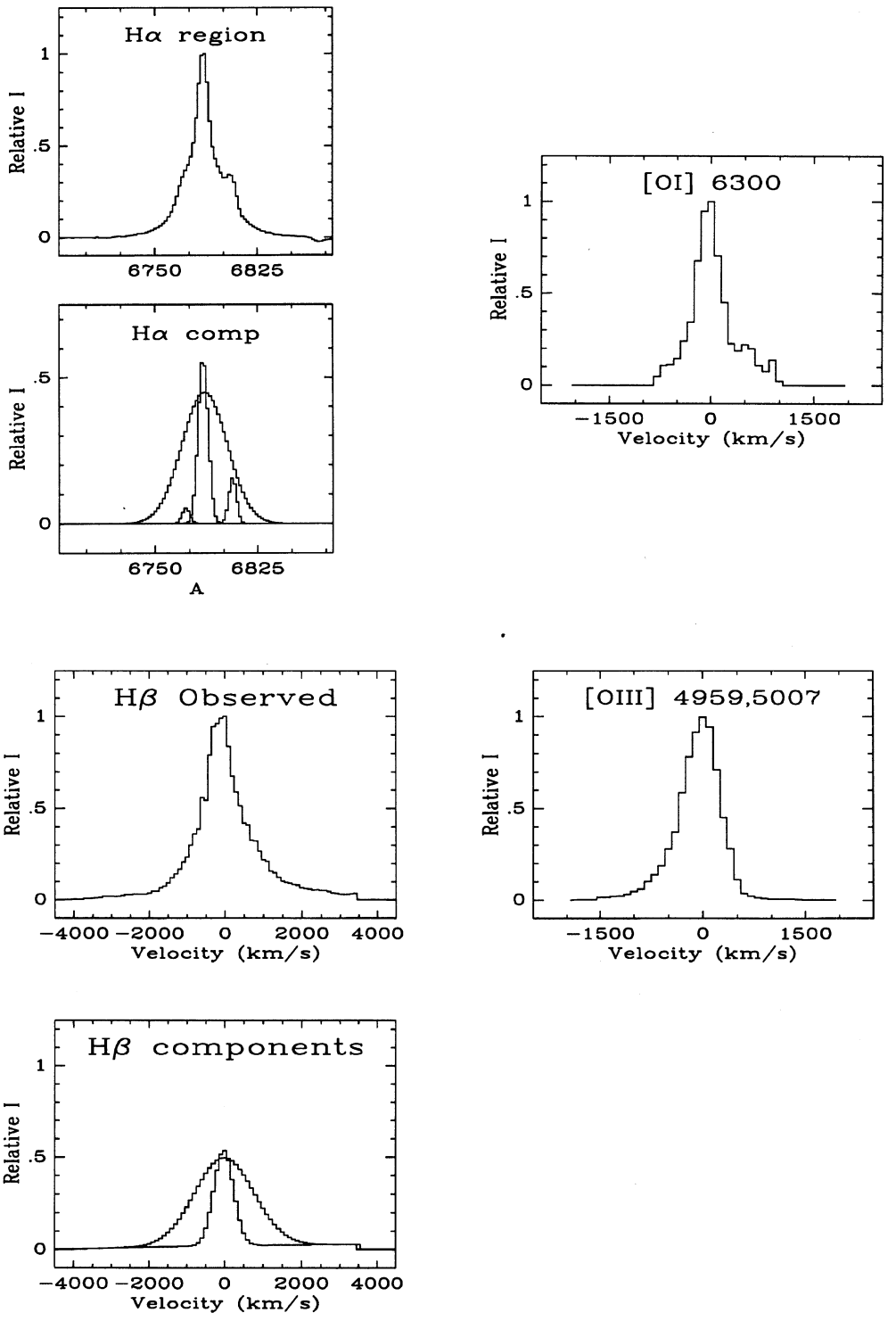

FIG. 4. Normalized profiles of the most interesting lines in the velocity space. The profile of Balmer lines can be represented by a composition of a broad component plus a narrow one. The [O III]4959, 5007 mean profile exhibits blueward asymmetry in the sense of being skewed to the red. [O I]6300 and He I 5876 show some evidence of a broad component, but it is only marginal due to the low signal to noise. The S II mean profile was constructed by normalizing and adding both lines and is representative of the instrumental profile. All the other lines show broader and asymmetric profiles.

© American Astronomical Society • Provided by the NASA Astrophysics Data System

1992AJ....104.1000Z

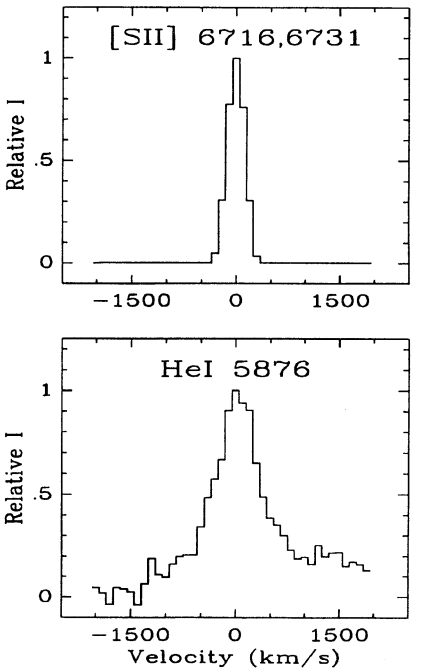

FIG. 4. (continued)

For measuring the peakness or stubbiness we have computed an additional parameter, the kurtosis K_1 defined by Whittle (1985) as

$$K_1 = 1.524 \frac{\text{FWHM}}{\text{FW}_{20}},$$

where FW_{20} is the full width at 20% intensity, which provides a value $K_1 = 0.91$ for the [O III] kurtosis.

In order to derive an estimation of the overall values of electron density and temperature, we used the model elaborated by Zamorano & Rego (1985). The line ratio [S II]6716/[S II]6731 $= 1.15 \pm 0.05$ is consistent with an electron density $N_e = 300$ cm^{-3}. The electron temperature was derived from the line intensity ratio [O III]4959 +5007/[O III]4363 $= 17 \pm 5$. The principal source of error in this ratio is the [O III]4363 line which appears blended with Hγ. In order to obtain a reliable value, a scaled Hβ line was used to match the Hγ. The final precision in the [O III]4363 line is estimated to be around 30%. Since the region where the [O III] lines are emitted in preference is much more ionized than the [S II] lines formatting region, a value of $N_e = 10\,000$ cm^{-3} was assumed in order to compute the electron temperature T_e. Due to the poor accuracy in the [O III]4363 flux measure, we can only give an estimation, resulting in a rather high value of $T_e = 55\,000$ K.

The presence of distinct non-Gaussian profiles in active nuclei may be strong evidence against a purely pressure supported velocity field in which the clouds move in a similar manner to the bulge stars. A tight correlation was found between the widths of the lines at one-half and one-fourth of maximum intensity by De Robertis & Osterbrock

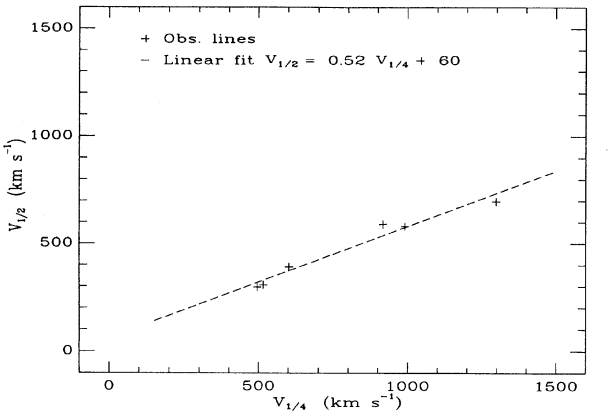

FIG. 5. Correlation of emission-line widths at half- and quarter-maximum intensities.

(1984). Such a correlation is also observed among the lines studied here (Fig. 5). In general

$$W_{50} = B \times W_{25} + A,$$

where $B = 0.52 \pm 0.01$ and $A = 60 \pm 10$. These values are similar to those found by De Robertis & Osterbrock (1984) with a similar velocity resolution. As they pointed out, such a correlation (with similar slope) is also observed in the broad component of Hβ profiles in Seyfert 1 galaxies and QSO's (De Robertis 1985). The ratios of widths at various relative intensities define the line profile and must be predicted by the proper geometry and acceleration mechanism for the narrow-line region (NLR). One interpretation of the similarity of the slope between our NLR data and the result for QSO is that the same acceleration mechanism may be operating throughout both central types of regions. Although their activities differ quantitatively, all the data are consistent with the next scenario for this object: the presence of lines of high ionized elements and the strong asymmetries in the [O III] lines suggest the existence of a high flow of turbulent material and a broad-line region (BLR) around a compact core. The observed emission suggests that the region of ionized material could be extended to the outer parts of the bulge, giving rise to an extended narrow-line region (ENLR).

3.2 Morphology

The analysis of the image that supports UCM 2257 +2438 is a $r = 15.88$ mag spiral galaxy seen almost face on. The central surface brightness for the disk component $\mu_0 = 17.6$ is brighter than the typical value for a spiral galaxy (see, e.g., Kent 1985). The apparent domination of the spheroidal component in the profile could be due to the existence of the intense Seyfert nucleus. Moreover, the bandpass of the Gunn–Thuan r filter employed could provide another possible explanation, because the continuum in this region is very weak and the Hα emission line dominates the spectrum. Furthermore, the Gunn–Thuan r im-

© American Astronomical Society • Provided by the NASA Astrophysics Data System

1992AJ....104.1000Z

age would be mainly showing the emission gas distribution of the galaxy rather than the star-light contribution. The bulge effective surface brightness value of 20.5 is typical of Sa–Sb systems. The effective radius r_e corresponding to μ_e is 2.3 arcsec. These values located UCM 2257+2438 above the mean relation found by Kent (1985) and near the early type galaxies region in his diagram ($\log r_e$, μ_e) indicating again the presence of a bright Seyfert nucleus. When the bulge to disk ratio is expressed in the form of bulge to total luminosity (B/T), we obtain B/T=0.42 which corresponds to a Sa type according to Simien & de Vaucouleurs (1986) and to a Sa–Sb type according to Kent (1985). Another method for the characterization of the light distribution is based in the concentration parameter defined as $c=5\log[r(0.8)/r(0.2)]$, where $r(0.2)$ and $r(0.8)$ are the radii which contain 20% and 80% of the total luminosity of the galaxy, respectively (Kent 1985). For UCM 2257 +2438 we have obtained $c=3.74$, a typical value for a Sb morphological type. It should be noted that the concentration parameter is independent of the adjusted profile. In summary, our results support the spiral structure of UCM 2257+2438 which is possibly a Sa galaxy. This morphology is typical of galaxies associated to Seyfert nuclei (Woltjer 1990). This result is also in accordance with the first conclusions of the multicolor photometry of a homogeneous sample of Seyfert 1 galaxies of Bonoli *et al.* (1989), who found that the bulge component is important in almost all the profiles, even when a pointlike nuclear component is included in the model. Their results confirm that Seyfert 1 nuclei are found in early type spiral galaxies in preference.

Over the past few years attempts have been made to relate morphological and emission line parameters on the basis that the emission line rise from a plasma in a rotating structure. Rees (1978) has indicated that under most circumstances such a rotating object should possess an angular momentum vector whose direction is the same as that surrounding the galaxy. If this is correct, the observed nuclear line-widths should correlate with the inclination of the plane of the galaxy on the sky, given by b/a if one assumes that the outer disks of the Seyfert are circular. The attempts carried out by different authors to correlate the permitted and forbidden line widths to the b/a axial relation have been unsuccessful. Only Simkin *et al.* (1980) found a tenuous relation between b/a and the Hβ width at zero intensity, using only 11 objects, which cannot be considered statistically significant. The axial relation of UCM 2257+2438, $b/a=0.80\pm0.02$, is slightly higher than the mean values for seven narrow-line Seyfert 1 galaxies, $b/a=0.65\pm0.11$ (Osterbrock & Pogge 1985).

3.3 Starlight (IR)

UCM 2257+2438 presents a near IR index $J-K=1.3\pm0.3$, which is typical of a Seyfert galaxy (Balzano & Weedman 1981). The $J-H$ and $H-K$ indices, when plotted in the Hyland & Allen (1982) diagram, where a combination of normal elliptical galaxies and nonthermal component is represented, point out a significant starlight contribution.

3.4 Far-Infrared Properties

The 60 to 25 μm far-infrared spectral index of UCM 2257+2438, $\alpha(60,25)=1.48$ is consistent with the Seyfert nature of the optical spectrum. The 60 μm luminosity was estimated as the product νL_ν, where L_ν is the luminosity density, which was computed assuming a deceleration parameter $q_0=1/2$, leading to a result $L(60\ \mu\text{m})=1.1\times10^{44}$ erg s^{-1} or $2.8\times10^{10}\ L_\odot$. No attempts were done to use the 100 μm flux because this value is contaminated by the emission from the nearest PSC source, as can be seen at the plot of the zone at this band (see Fig. 6).

A detailed comparison of the plots of the UCM galaxy at all four *IRAS* bands against the *IRAS* source at the south shows the different behavior of a normal object (U12290, a normal spiral galaxy) and our Seyfert. An arrow labeled "1" points to the optical position of UCM 2257+2438. Another arrow labeled "2" points to U12290. The PSF of the instrument originates the elongated shape of the images. Only the normal galaxy is partially resolved.

At 12 μm the brightness of the two objects is more or less the same. Both of them show significant contribution of an old component star population (the 12 μm emission is usually originated by hot dust in, or at least very near H II regions; see, e.g., Natta & Panagia 1976). At 25 μm the UCM galaxy is stronger, because at 25 μm the main contribution is due to reemission of high ionizing photons by dust. The nonthermal component gives rise to a bright nuclei seen at this band. The 60 μm emission is assumed from reemission of both ionizing and nonionizing photons. That is why the *IRAS* source, as a big normal spiral galaxy, is stronger at this image. The disk contribution of the UCM's parent galaxy is also shown. Finally, due to the poor *IRAS* resolution at 100 μm (around 4 arcmin), the emission from both galaxies at this band is mixed. There is also superimposed a cirrus background from our own galaxy. A good determination of the 100 μm fluxes was not possible.

4. CONCLUSIONS

UCM 2257+2438 is a new Sa galaxy, with a redshift $z=0.0337\pm0.0001$, which harbors a narrow-line Seyfert 1 nucleus. The surface brightness profile of the Gunn–Thuan r image seems to be dominated by a spheroidal component, probably due to the nuclear activity. Its optical spectra is similar to the spectra of narrow-line galaxies (Osterbrock & Shaw 1988) with an internal reddening, based on the Balmer decrement, $E(B-V)=0.54$.

The Balmer lines of hydrogen are easily deblended in broad and narrow components. They also exhibit extended wings with a full width at zero intensity of $=6000$ km s^{-1}. The [O III] lines show marked blueward asymmetries. The narrow-line region gas has an average velocity dispersion of 250 km s^{-1} with a rather high electron temperature of about 55 000 K (assuming a electron density $N_e=10\,000$

© American Astronomical Society • Provided by the NASA Astrophysics Data System

1992AJ....104.1000Z

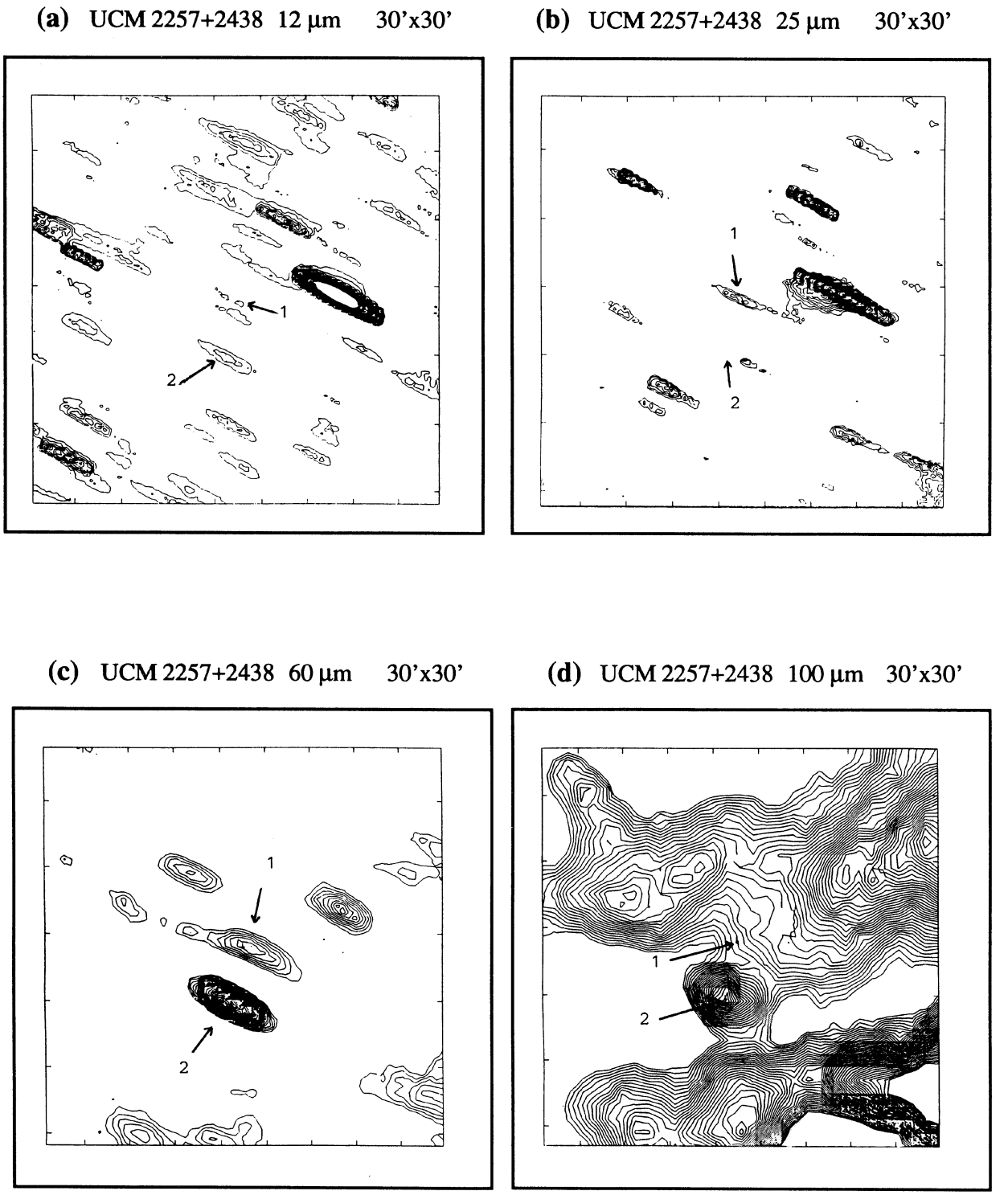

FIG. 6. The contour plots for each of the *IRAS* bandpasses for (1) UCM 2257+2438 and (2) UGC 12290. The elongated contours are a result of the rectangular shape of the *IRAS* detectors.

© American Astronomical Society • Provided by the NASA Astrophysics Data System

1992AJ....104.1000Z

cm^{-3}). A tight correlation between the widths at 25% and 50% intensity is found for the emission lines, with values similar to those reported previously by other authors. All the spectral information suggests that the ionized material is extended.

An analysis of *IRAS* images in the neighborhood of UCM 2257+2438 has been carried out. The presence of a normal galaxy permits us to compare the different behavior of both galaxies at each *IRAS* band.

Spectroscopic observations at both high spectral and spatial resolution could confirm our guess of the existence of a extended narrow-line region.

This work was supported in part by the Spanish "Programa Sectorial de Promocion General del Conocimiento" under Grant No PB89-124. The authors wish to thank an anonymous referee for his valuable comments and suggestions.

REFERENCES

Balzano, V. A., & Weedman, D. W. 1981, ApJ, **243**, 756
Bonoli, C., Bonoli, F., Danese, L., Delpino, F., DeZotti, G., Granato, G., & Zitelli, V. 1989, in Active Galactic Nuclei, IAU Symposium No. 134, edited by D. E. Osterbrock and J. S. Miller (Kluwer, Dordrecht), p. 49
Burstein, D., & Heiles, C. 1984, ApJS, **54**, 33
Davis, L. E., Cawson, M., Davies, R. L., & Illingworth, G 1985, AJ, **90**, 169
DeRobertis, M. M. 1985, ApJ, **289**, 67
DeRobertis, M. M., & Osterbrock, D. E. 1984 ApJ, **286**, 171
de Vaucoleurs, G. 1948, Annales d' Astrophysique, **11**, 247
Dixon, R. S., & Sonneborn, G. 1980, A Master List of Nonstellar Optical Astronomical Objects (Ohio State University Press, Columbus)
Freeman, K. 1970, ApJ, **160**, 811
Hyland, A. R., & Allen, D. A. 1982, MNRAS, **199**, 943
Kazarian, M. A., & Kazarian, E. S. 1980, Afz, **16**, 17
Kent, S. M. 1985, PASP, **97**, 165
Koski, A. T. 1978, ApJ, **223**, 56
Natta, A., & Panagia, N. 1976, A&A, **50**, 191
Neltzer, J. A. & Mead, R. 1965, Computer Journal No. **7**, 308
Osterbrock, D. E. 1977, ApJ, **215**, 733
Osterbrock, D. E., & Pogge, R. W. 1985, ApJ, **297**, 166
Osterbrock, D. E., & Shaw, R. A. 1988, ApJ, **327**, 89
Osterbrock, D. E., 1989, Astrophysics of Gaseous Nebulae and Active Galactic Nuclei (University Science Books, Mill Valley)
Paturel, G., Fouqué, P., Bottinelli, L., & Gouguengheim, L. 1989, A&AS, **80**, 299
Rego, M., Zamorano, J., & González-Riestra, R. 1989, A&AS, **62**, 173
Rees, M. J. 1978, Nature, **275**, 516
Schombert, J. M., & Bothun, G. D. 1987, AJ, **93**, 60
Simien, F., & de Vaucouleurs, G. 1986, ApJ, **302**, 564
Simkin, S. M., Su, H. J. & Schwarz, M. P. 1980, ApJ, **237**, 404
Whittle, M. 1985, MNRAS, **213**, 1
Woltjer, L. 1990, in Active Galactic Nuclei, Saas-Fee Advanced Course No. 20, edited by R. D. Blandford, H. Netzer, and L. Woltjer (Springer, Berlin), p. 1
Zamorano, J., & Rego, M. 1985, A&AS **62**, 173
Zamorano, J., Rego, M., & González-Riestra, R. 1990, Ap&SS, **170**, 353

© American Astronomical Society • Provided by the NASA Astrophysics Data System